

Color Imaging: Device - Independent
Color, Color Hardcopy, &
Applications VII

Vol. 4668



PROCEEDINGS OF SPIE
SPIE—The International Society for Optical Engineering

Color Imaging: Device-Independent Color, Color Hardcopy, and Applications VII

**Reiner Eschbach
Gabriel G. Marcu**
Chairs/Editors

**22–25 January 2002
San Jose, USA**

Sponsored by
IS&T—The Society for Imaging Science and Technology
SPIE—The International Society for Optical Engineering

Published by
SPIE—The International Society for Optical Engineering



Volume 4663

SPIE is an international technical society dedicated to advancing engineering and scientific applications of optical, photonic, imaging, electronic, and optoelectronic technologies.



The papers appearing in this book compose the proceedings of the technical conference cited on the cover and title page of this volume. They reflect the authors' opinions and are published as presented, in the interests of timely dissemination. Their inclusion in this publication does not necessarily constitute endorsement by the editors or by SPIE. Papers were selected by the conference program committee to be presented in oral or poster format, and were subject to review by volume editors or program committees.

Please use the following format to cite material from this book:

Author(s), "Title of paper," in *Color Imaging: Device-Independent Color, Color Hardcopy, and Applications VII*, Reiner Eschbach, Gabriel G. Marcu, Editors, Proceedings of SPIE Vol. 4663, page numbers (2002).

ISSN 0277-786X
ISBN 0-8194-4403-0

Published by
SPIE—The International Society for Optical Engineering
P.O. Box 10, Bellingham, Washington 98227-0010 USA
Telephone 1 360/676-3290 (Pacific Time) • Fax 1 360/647-1445
<http://www.spie.org/>

Copyright© 2002, The Society of Photo-Optical Instrumentation Engineers.

Copying of material in this book for internal or personal use, or for the internal or personal use of specific clients, beyond the fair use provisions granted by the U.S. Copyright Law is authorized by SPIE subject to payment of copying fees. The Transactional Reporting Service base fee for this volume is \$15.00 per article (or portion thereof), which should be paid directly to the Copyright Clearance Center (CCC), 222 Rosewood Drive, Danvers, MA 01923 USA. Payment may also be made electronically through CCC Online at <http://www.directory.net/copyright/>. Other copying for republication, resale, advertising or promotion, or any form of systematic or multiple reproduction of any material in this book is prohibited except with permission in writing from the publisher. The CCC fee code is 0277-786X/02/\$15.00.

Printed in the United States of America.

Conference Committee

Conference Chairs

Reiner Eschbach, Xerox Corporation (USA)
Gabriel G. Marcu, Apple Computer, Inc. (USA)

Program Committee

Jan Bares, NexPress Solutions, LLC (USA)
Makoto Fujino, Seiko Epson Corporation (Japan)
Roger-David Hersch, Ecole Polytechnique Fédérale de Lausanne (Switzerland)
Patrick G. Herzog, RWTH-Aachen (Germany) and Color AlXperts GmbH (Germany)
Hiroaki Ikegami, Fuji Xerox Company, Ltd. (Japan)
Jae Ho Kim, Pusan National University (Korea)
Helmut Kipphan, Heidelberger Druckmaschinen AG (Germany)
Michael A. Kriss, Sharp Laboratories of America
Shaun T. Love, Lexmark International, Inc. (USA)
Chris Tuijn, Agfa-Gevaert N.V. (Belgium)
John C. Urbach, Consultant (USA)

Session Chairs

- 1 Spectral Imaging I
Reiner Eschbach, Xerox Corporation (USA)
- 2 Spectral Imaging II
Gabriel G. Marcu, Apple Computer, Inc. (USA)
- 3 Color Perception
Reiner Eschbach, Xerox Corporation (USA)
- 4 Image Processing
Jan Bares, NexPress Solutions, LLC (USA)
- 5 Color Reproduction
Shaun T. Love, Lexmark International, Inc. (USA)
- 6 Displays
A. Ufuk Agar, Hewlett-Packard Laboratories (USA)
- 7 Color Management
Gabriel G. Marcu, Apple Computer, Inc. (USA)
- 8 Halftoning
Jan P. Allebach, Purdue University (USA)

- 9 Halftoning II
Reiner Eschbach, Xerox Corporation (USA)

Contents

vii *Conference Committee*

SESSION 1 SPECTRAL IMAGING I

- 1 **Innovative method for spectral-based printer characterization [4663-02]**
S. Zuffi, R. Schettini, CNR (Italy)

SESSION 2 SPECTRAL IMAGING II

- 8 **Spectrum recovery from colorimetric data for color reproductions [4663-03]**
G. Sharma, S. Wang, Xerox Corp. (USA)
- 15 **Color image reproduction based on multispectral and multiprimary imaging: experimental evaluation [4663-04]**
M. Yamaguchi, Tokyo Institute of Technology (Japan) and Telecommunications Advancement Organization of Japan; T. Teraji, Tokyo Institute of Technology (Japan); K. Ohsawa, T. Uchiyama, H. Motomura, Telecommunications Advancement Organization of Japan; Y. Murakami, N. Ohya, Tokyo Institute of Technology (Japan) and Telecommunications Advancement Organization of Japan
- 27 **Recording and rendering for art paintings based on multiband data [4663-05]**
S. Tominaga, N. Tanaka, T. Matsumoto, Osaka Electro-Communication Univ. (Japan)

SESSION 3 COLOR PERCEPTION

- 35 **Factors effecting lightness partitioning [4663-07]**
N. Moroney, Hewlett-Packard Labs. (USA)
- 43 **Refinement of a model for predicting perceived brightness [4663-08]**
U. Eisemann, RWTH-Aachen (Germany)
- 51 **3D histograms in color image reproduction [4663-09]**
P.-L. Sun, J. Morovic, Univ. of Derby (UK)

SESSION 4 IMAGE PROCESSING

- 63 **Simple segmentation algorithm for mixed raster contents image representation [4663-10]**
Z. Fan, M. Xu, Xerox Corp. (USA)
- 72 **Color document analysis [4663-11]**
C. Kuo, NexPress Solutions LLC (USA); A. R. Rao, G. Thompson, IBM Thomas J. Watson Research Ctr. (USA)
- 81 **Picture/graphics classification using texture features [4663-12]**
Z. Fan, R. Bala, Xerox Corp. (USA)

- 86 **Rate-distortion-based segmentation for MRC compression** [4663-13]
H. Cheng, Sarnoff Corp. (USA); G. Feng, C. A. Bouman, Purdue Univ. (USA)
- 98 **Recent progress in automatic digital restoration of color motion pictures** [4663-14]
M. Chambah, B. Besserer, P. Courtellemont, Univ. de La Rochelle (France)

SESSION 5 COLOR REPRODUCTION

- 110 **Color gamut reduction techniques for printing with custom inks** [4663-15]
S. M. Chosson, R. D. Hersch, Ecole Polytechnique Fédérale de Lausanne (Switzerland)
- 121 **Measurement-based printer models with reduced number of parameters** [4663-16]
K. R. Crouse, Agfa Monotype Corp. (USA)
- 130 **How to ensure consistent color quality in inkjet proofing** [4663-17]
S. Livens, M. F. Mahy, D. Vansteenkiste, Agfa-Gevaert NV (Belgium)
- 137 **Determining the source of unknown CMYK images** [4663-18]
R. Bala, Xerox Corp. (USA)
- 143 **CMYK transformation with black preservation in color management system** [4663-19]
H. Zeng, Hewlett-Packard Co. (USA)
- 150 **Modeling a CMYK printer as an RGB printer** [4663-20]
J. Z. Chang, J. C. Dalrymple, Sharp Labs. of America

SESSION 6 DISPLAYS

- 162 **Color: an exosomatic organ? (Invited Paper)** [4663-06]
J. van Brakel, Katholieke Univ. Leuven (Belgium), B. Saunders, Univ. of Cambridge (UK)
- 177 **Comparative evaluation of color characterization and gamut of LCDs versus CRTs** [4663-23]
G. Sharma, Xerox Corp. (USA)
- 187 **Color characterization issues for TFTLCD displays** [4663-24]
G. G. Marcu, W. Chen, K. Chen, P. Graffagnino, O. Andrade, Apple Computer, Inc. (USA)

SESSION 7 COLOR MANAGEMENT

- 199 **Network color management system using a cluster dividing method** [4663-25]
M. Nichogi, K. Kanamori, Matsushita Electric Industrial Co., Ltd. (Japan)
- 207 **Primary preservation in ICC color management system** [4663-27]
H. Zeng, Hewlett-Packard Co. (USA)
- 217 **Appearance match between hardcopy and softcopy using lightness rescaling with black point adaptation** [4663-28]
K. Nakabayashi, Sony Corp. (Japan); M. D. Fairchild, Rochester Institute of Technology (USA)

SESSION 8 HALFTONING

- 229 **Stochastic dithering and watermarking (Invited Paper)** [4663-29]
C. L. Nino, G. R. Arce, Univ. of Delaware (USA)
- 242 **Halftone screen encoding methods** [4663-30]
H. R. Kang, Aetas Technology Inc. (USA)
- 250 **Compression of screened halftone image using block prediction** [4663-31]
X. Feng, Sharp Labs. of America
- 257 **High-speed multilevel halftoning hardware** [4663-32]
M. T. Brady, C. H. Morris III, IBM Corp. (USA); J. L. Mitchell, IBM Thomas J. Watson Research Ctr. (USA)
- 264 **Multilevel screen design using direct binary search** [4663-33]
G.-Y. Lin, J. P. Allebach, Purdue Univ. (USA)

SESSION 9 HALFTONING II

- 278 **New methods for digital halftoning and inverse halftoning** [4663-35]
M. Meşe, P. P. Vaidyanathan, California Institute of Technology (USA)
- 293 **Error diffusion with blue-noise properties for midtones** [4663-36]
P.-M. Jodoin, V. Ostromoukhov, Univ. de Montréal (Canada)
- 302 **Fast error diffusion** [4663-37]
H. R. Kang, Aetas Technology Inc. (USA)
- 310 **Tone-dependent error diffusion** [4663-38]
P. Li, Sony Electronics Inc. (USA); J. P. Allebach, Purdue Univ. (USA)
- 322 **AM/FM halftoning: a method for digital halftoning through simultaneous modulation of dot size and dot placement** [4663-39]
Z. He, C. A. Bouman, Purdue Univ. (USA)

POSTER SESSION

- 335 **Thermo autochrome printer TPH heating compensation method** [4663-40]
Y.-H. Wu, H.-J. Tsai, Industrial Technology Research Institute (Taiwan)
- 343 **Fundamental study on electromechanics of particles for printing technology** [4663-41]
H. Kawamoto, N. Nakayama, Waseda Univ. (Japan)
- 355 **Analysis of capacitance sensitivity distributions and image reconstruction in electrical capacitance tomography** [4663-42]
D. Chen, G. Zheng, X. Yu, Harbin Univ. of Science and Technology (China); Y. Wang, T. Zhou, Heilongjiang Provincial Metrology Institute (China)
- 360 **Parallel error diffusion** [4663-43]
H. R. Kang, Aetas Technology Inc. (USA)

370 **Development of goniophotometric imaging system for recording reflectance spectra of 3D objects [4663-44]**
K. Tonsho, Y. Akao, N. Tsumura, Y. Miyake, Chiba Univ. (Japan)

380 *Author Index*

An innovative method for spectral-based printer characterization

Silvia Zuffi, Raimondo Schettini*

Istituto Tecnologie Informatiche Multimediali, Consiglio Nazionale delle Ricerche
Via Ampere 56, 20131 Milano, Italy

ABSTRACT

The paper presents an innovative approach to the spectral-based characterization of ink-jet color printers. Our objective was to design a color separation procedure based on a spectral model of the printer, managed here as an RGB device. The printer was a four-ink device, and we assumed that the driver always replaced the black completely when converting from RGB to CMYK amounts of ink. The color separation procedure, which estimates the RGB values given a reflectance spectrum, is based on the inversion of the Yule-Nielsen modified Neugebauer model. To improve the performance of the direct Neugebauer model in computing the reflectance spectrum of the print, given the amounts of ink, we designed a method that exploits the results of the numerical inversion of the Neugebauer model to estimate a correction of the amount of black ink computed on RGB values. This correction can be considered a first step in optimization of the Neugebauer model; it accounts for ink-trapping and the lack of knowledge on how the black is actually replaced by the printer driver.

Keywords: Color printer model, spectral-based printer characterization, Neugebauer model, inkjet printers.

1. INTRODUCTION

Many models have been proposed to describe the color behavior of printers analytically. One of the first attempts to predict the outcome of a halftone printing process was the extension introduced by Neugebauer in 1937 of the monochrome Murray-Davies model. The further addition of the empirical Yule-Nielsen n -value to account for light scattering effects produced the frequently used Yule-Nielsen modified Neugebauer model¹. The accuracy of this model has been investigated by Rolleston and Balasubramanian². The Yule-Nielsen modified Neugebauer model does not account for physical interaction among inks, and some techniques to cope with this problem have recently been presented. Stollnitz et al.³ have added ink trapping to the Neugebauer equations, while Iino and Berns⁴ and Tzeng⁵ have used a second order improvement technique to model ink and optical trappings.

An accurate description of the color behavior of a printer is necessary, but not sufficient for spectral-based characterization. Another important issue is the inversion of the mathematical model that describes the printing process, in order to obtain the digital controls that enable the printer to reproduce, with the greatest possible accuracy, a given reflectance spectrum. Only the three-ink Neugebauer model can be inverted analytically: a scheme for this inversion has been proposed by Mahy and Delabastita⁶. Praefcke⁷ has evaluated two approaches to color separation, among which the iterative inversion of the Yule-Nielsen modified Neugebauer model. Iino and Berns⁸ have used two models to characterize ink-jet printers: the spectral Murray-Davies-Yule-Nielsen with n -value dependent from the wavelength, and the Omatsu model. They have evaluated two approaches for model inversion, the Newton-Raphson, a derivative-based method, and the Simplex method, observing that the Simplex method is preferable, as it eliminates the need to compute derivatives on measured data. A six-inks spectral-based color separation has been presented by Tzeng and Berns⁹.

We have address the problem of the spectral-based characterization of a four-ink inkjet printer. Our objective was to design a color separation procedure based on a spectral model of the printer, managed here as an RGB device. We present here an innovative way of improving the performance of the Yule-Nielsen modified Neugebauer model which we used to describe the device analytically. To improve the performance of the direct Neugebauer model in computing the reflectance spectrum of the print, given the amounts of ink, we have designed a method that exploits the results of the numerical inversion of the Neugebauer model to estimate a correction of the amount of black ink computed from

* [zuffi, schettini]@itim.mi.cnr.it

RGB. We have considered only the black ink for two reasons: first, in many practical cases how the printer driver computes the amount of black may not be known; second, as the black ink is printed last, it is the ink most influenced by the presence of the other inks. The correction based on the black ink is therefore a first step in improving the Neugebauer model, accounting for ink-trapping and lack of knowledge on how the black is actually replaced by the printer driver.

2. THE PRINTER MODEL

According to the spectral Neugebauer model, the spectrum of a n -inks halftone print is the weighted summation of 2^n different colors, called Neugebauer primaries, given by all the possible overprints of inks. The weight of each Neugebauer primary is the area it covers in the halftone cell. Yule and Nielsen have proposed a correction that was applied to the Neugebauer model¹⁰ to account for the optical dot gain effect due to the scattering of light in paper. The Yule-Nielsen modified Spectral Neugebauer (YNSN) model for a 4-ink halftone print is:

$$R_{print,\lambda} = \left[\sum_{p=0}^{15} a_p R_{p,\lambda}^n \right]^n \tag{1}$$

where $R_{print,\lambda}$ is the reflectance of the printed color, n is the Yule-Nielsen factor, $R_{p,\lambda}$ is the reflectance of the p -th Neugebauer primary, and a_p is the primary area coverage. The area coverage of each Neugebauer primary is computed using Demichel's dot overlap model.

$$a_p = \prod_{i=0}^3 [ind_{p,i} c_i + (1 - ind_{p,i})(1 - c_i)] \quad p = 0 \dots 15 \quad \mathbf{c} = [c, m, y, k] \tag{2}$$

where c_i represents the area covered by the i -th ink dot in the halftone cell, and ranges from 0 (absence of ink) to 1 (full ink coverage). And $ind_{p,i}$ is the digit of position i of the index of the primary p , when p is expressed in binary code and the primaries are in the order: white ($ind_0=[0,0,0,0]$), black ($ind_1=[0,0,0,1]$), yellow ($ind_2=[0,0,1,0]$), yellow and black ($ind_3=[0,0,1,1]$), magenta ($ind_4=[0,1,0,0]$), magenta and black ($ind_5=[0,1,0,1]$), red ($ind_6=[0,1,1,0]$), red and black ($ind_7=[0,1,1,1]$), cyan ($ind_8=[1,0,0,0]$), cyan and black ($ind_9=[1,0,0,1]$), green ($ind_{10}=[1,0,1,0]$), green and black ($ind_{11}=[1,0,1,1]$), blue ($ind_{12}=[1,1,0,0]$), blue and black ($ind_{13}=[1,1,0,1]$), cyan, magenta and yellow ($ind_{14}=[1,1,1,0]$), four inks ($ind_{15}=[1,1,1,1]$).

We assume, for the dot overlap model to hold, that the dots are printed randomly, and are rectangular in cross section. In reality, dots have soft transitions, and in cases of high frequency rotated screens or error diffusion, much of the paper is covered by transitory regions. In these cases the experimentally computed Yule-Nielsen factor, estimated to account for optical dot gain, also accounts for soft transitions, exceeding the theoretical limit of 2^{11} .

We have considered the printer an RGB device; therefore the theoretical areas of dots are expressed as function of RGB values. Ink concentrations and digital counts for a four-ink printer are expressed accordingly by the following equations¹²:

$$\begin{aligned} c &= c' - U \cdot k, \\ m &= m' - U \cdot k, \\ y &= y' - U \cdot k, \\ k &= R \cdot \min(c', m', y'), \\ 0 &\leq R \leq 1, 0 \leq U \leq 1 \end{aligned} \tag{3}$$

where $c' = 1 - r, m' = 1 - g, y' = 1 - b$.

In our experiment we set $U=R=1$.

The effective size of a dot printed on a substrate is larger than its theoretical size, due to the spread of the ink on the paper. This effect is referred to as mechanical dot gain, and is modeled by experimentally computed dot-gain functions.

For ink i , we indicate with f_i the dot-gain function, with $c_{i,t}$ the theoretical dot area, with c_i the effective dot area, with $\varphi_i(\mathbf{r})$ the function that coded equation (3), and with \mathbf{r} the vector of the RGB values normalized in the range of [0,1]. In formulae:

$$c_i = f_i(c_{i,t}), \quad \text{where} \quad c_{i,t} = \varphi_i(\mathbf{r}) \quad \mathbf{r} = [r, g, b] \quad \mathbf{c} = [c, m, y, k] \quad (4)$$

In our application dot-gain functions are actually estimated for the inks and for the secondary colors, red, green and blue, and are applied as follows:

$$\begin{aligned} r_t &= \min(m_t, y_t) & g_t &= \min(c_t, y_t) & b_t &= \min(m_t, c_t) \\ c_t' &= c_t - g_t - b_t & m_t' &= m_t - r_t - b_t & y_t' &= y_t - r_t - g_t \end{aligned} \quad (5)$$

$$\begin{aligned} c &= f_c(c_t') + f_g(g_t) + f_b(b_t) & m &= f_m(m_t') + f_r(r_t) + f_b(b_t) & y &= f_y(y_t') + f_r(r_t) + f_g(g_t) \\ k &= f_k(k_t) \end{aligned}$$

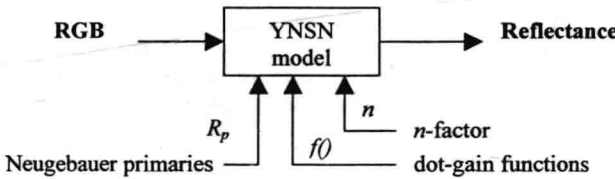


Figure 1. Scheme of the direct printer model. The parameters for the model are the Neugebauer primaries (R_p), the dot-gain functions ($f()$), and the Yule-Nielsen factor (n).

3. PRINTER MODEL INVERSION

The inversion of the YNSN model cannot be performed analytically; the solution must be numerically estimated. To do so, we use the Levenberg-Marquardt (L-M) method¹³, which finds a solution that minimizes a cost function, which we define as follows:

$$\chi^2(\mathbf{r}) = \sum_{\lambda} \frac{[R_{original,\lambda} - R_{print,\lambda}(\mathbf{r})]^2}{\sigma_{\lambda}^2} \quad \sigma_{\lambda} = \frac{1}{I_{D65,\lambda}} \quad (6)$$

where $R_{original,\lambda}$ is the input reflectance, $R_{print,\lambda}$ is the reflectance computed using equation (1), \mathbf{r} is the r, g, b vector, and σ_{λ} is the $R_{original,\lambda}$ standard deviation. We set σ_{λ} as the inverse of the D65 illuminant spectrum to weight the error at each wavelength on the basis of the relevance of the corresponding reflectance value when the color is observed under daylight conditions. The L-M recipe requires the computation of the partial derivative of the estimated reflectance with respect to the \mathbf{r} vector.

$$\frac{\partial R_{print,\lambda}}{\partial r_k} = n \cdot \left[\sum_{p=0}^{15} a_p R_{p,\lambda}^n \right]^{n-1} \cdot \sum_{p=0}^{15} \frac{\partial a_p}{\partial r_k} R_{p,\lambda}^n \quad (7)$$

If, for simplicity, we define in equation (2) $A_{p,i} = ind_{p,i} \cdot c_i + (1 - ind_{p,i}) \cdot (1 - c_i)$, then the partial derivative of the area coverage can be computed as follows:

$$\frac{\partial a_p}{\partial r_k} = \sum_{h=0}^3 \left[\frac{\partial A_{p,h}}{\partial r_k} \cdot \prod_{\substack{i=0 \\ i \neq h}}^3 A_{p,i} \right] \quad \text{with} \quad \frac{\partial A_{p,h}}{\partial r_k} = \text{ind}_{p,h} \frac{\partial f_h(\varphi_h(\mathbf{r}))}{\partial r_k} - \left(1 - \text{ind}_{p,h} \frac{\partial f_h(\varphi_h(\mathbf{r}))}{\partial r_k} \right) \quad (8)$$

That is, for the separation procedure the first derivative of the dot-gain functions $f()$ and the dependence of the ink concentrations, expressed by $\varphi()$, must be computed with respect to the digital counts that drive the printer (\mathbf{r}). For the L-M iterative method an initial solution must be assigned. This was set at medium gray. Moreover, to guarantee feasible solutions, when the method converges toward an out-of-gamut solution, at each iteration out of range r , g , and b values are clipped to a range of $[0, 1]$.

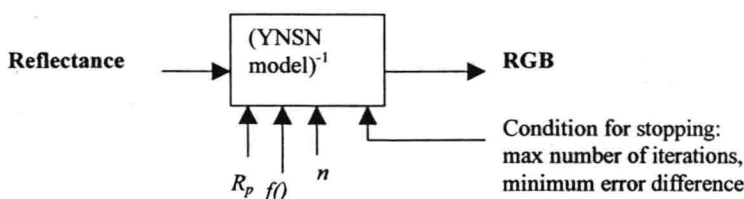


Figure 2. Scheme of the inverse printer model. The parameters for the model are the Neugebauer primaries (R_p), the dot-gain functions ($f()$) and the Yule-Nielsen factor (n). The L-M iterative method requires a condition for stopping, which has been set at a maximum number of iterations, or a minimum difference in the decrease of the cost function.

4. PRINTER MODEL APPLICATION AND IMPROVEMENT

In our experiment we employed an Epson Stylus Color printer, Floyd Steinberg dithering and Epson high quality paper. Measurements of spectra were performed using a Gretag Spectrolino, considering values in the wavelength range of 400 to 700 nm with a step of 10 nm. The Neugebauer primaries were obtained by measuring the printed inks at full coverage and their overprints, obtained by successive prints on the same sheet.

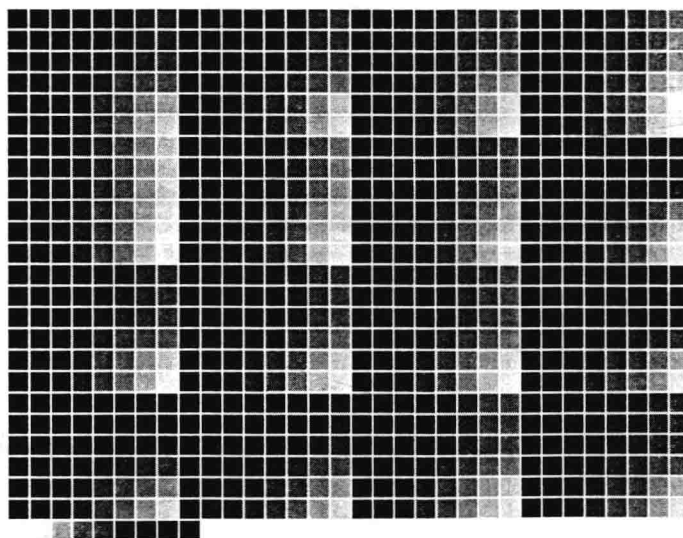


Figure 3. The test specimen, composed of 777 RGB colors representing a uniform sampling of the RGB space.

The Yule-Nielsen n -factor was obtained with an iterative procedure: a specimen composed of the ramps of the four inks was printed and measured. The measured spectra were compared with the spectra computed using the YNSN model for a set of values of n , ranging from 1 to 20 with a step of 0.1. The lowest of the means of the color distance units between the measured and the computed reflectance gave the best n -value estimate of 10.3.

Once the n -factor was defined, dot-gain functions were estimated for the four inks and for the three secondary colors red, green and blue; to do so a specimen composed of the ramps of cyan, magenta, yellow, red, green, blue and black was printed and measured. Least square regression was used to compute the effective area coverage for each sample, using the Murray-Davies model¹⁴. Dot-gain functions $f()$ are fourth order polynomials that interpolate between computed effective areas of coverage.

The specimen used to test the direct printer model was composed of 777 colors by uniformly sampling the RGB color space (see Figure 3). The RGB values of the test specimen were given as the input to the printer model to compute the 777 reflectance spectra; the difference between the measured and the computed spectra was then quantified in color distance units. The values of the mean, maximum and standard deviation are reported in Table 1.

4.1 Printer model improvement

Our analysis of the computed reflectance spectra indicated that the YNSN model was inappropriate for predicting the reflectance of colors generated with more than one ink. This failure could be ascribed to the presence of a more complex dot gain effect when multiple inks coexist. A further reason could be the mismatch between the actual and the hypothesized algorithm converting RGB into inks concentrations. To improve the accuracy of the direct model we designed a procedure that could better compute the effective dot area of the black ink. We focused on the black ink principally for two reasons: first, how the printer driver actually manages the amount of black is generally an unknown; second, we expect the black ink to be printed last¹², and we may therefore assume that it is the ink most influenced by the presence of the other inks.

To improve the model's performance, we proceeded as follows. We printed the ramps of cyan, magenta and yellow from full ink to black. Consequently in each ramp the concentration of ink ranged from 1 to 0, while the concentration of black ranged from 0 to 1. We measured the printed image, and then used the reflectance spectra of the ramps of the three inks as input for the separation procedure to estimate the amount of black ink in each patch. The estimated concentrations of black in the ramps of cyan, magenta and yellow are plotted in Figure 4. The separation procedure estimates an amount of black exceeding the theoretical value, with similar behavior for the three inks.

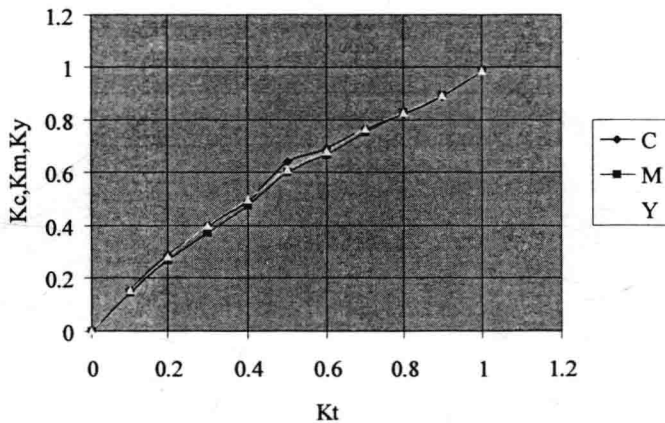


Figure 4. Plot of the theoretical concentration of black computed using equation (3) compared with the theoretical concentration of black estimated with the inverse model for ramps of cyan, magenta and yellow from full ink to black. In each ramp the concentration of ink ranged 1 to 0, while the concentration of black ranged from 0 to 1.

We defined as ‘black gain’ (g_k) the difference between the estimated and the theoretical concentration of black (k_t), where the estimated value is the mean for the three inks:

$$g_k(k_t) = \text{mean}(k_c, k_m, k_y) - k_t \tag{9}$$

The black-gain, represented as a fourth order polynomial, was used to compute the effective dot area of black as follows:

$$k = f_k(k_t + (c_t + m_t + y_t + k_t) \cdot g_k(k_t)) \tag{10}$$

Summarizing, the printer model definition consists in the estimation of the n -factor, dot-gain functions, and black-gain, as shown in Figure 5.

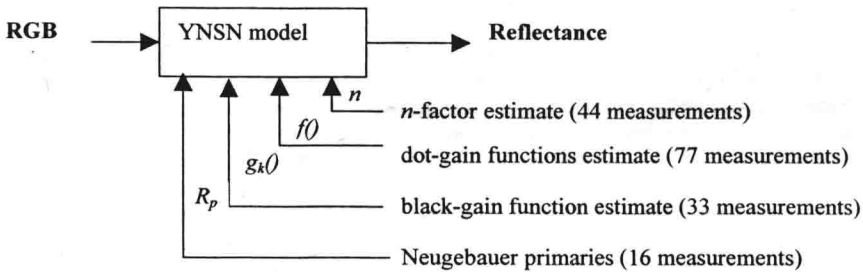


Figure 5. Scheme of the direct printer model defined with a total of 126 spectral measurements.

To verify the improvement in the printer model brought by introducing the correction described, the reflectance spectra for the specimen were computed; the statistics of the resulting color distance units are indicated in Table 1. Figure 6 gives the measured reflectance spectrum of the fifth sample of the specimen together with the spectrum computed by applying the YNSN model without and with the correction for black-gain.

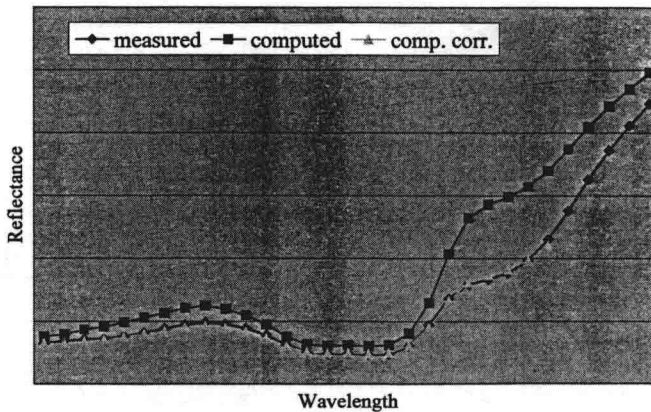


Figure 6. An example of the improvement in the estimation of the printed reflectance spectrum for the sample RGB=160,0,0. The measured reflectance (‘measured’) is plotted together with the reflectance computed with the direct model without correction for black-gain (‘computed’), and with (‘comp. corr.’).

YNMN model	Mean		Maximum		Std deviation	
	ΔE_{94}	ΔE_{ab}	ΔE_{94}	ΔE_{ab}	ΔE_{94}	ΔE_{ab}
without correction	3.25	3.65	9.83	14.60	2.30	2.76
with correction	1.53	1.78	6.41	8.84	0.81	1.06

Table 1. Statistics of the color distance units between the measured and the computed reflectance spectra for the specimen of Figure 3 without and with black-gain correction.

5. CONCLUSIONS

We have presented a procedure for the spectral characterization of a four-ink inkjet printer treated as an RGB device. Starting from the Yule-Nielsen modified Spectral Neugebauer model, a well-known mathematical model that describes the reflectance of an halftone print, we have designed a method for optimizing its performance. Using this method we have been able to characterize a printer with about 130 spectral measurements and an error of 1.8 cdu.

REFERENCES

1. D. R. Wyble, R. S. Berns, "A Critical Review of Spectral Models Applied to Binary Color Printing", *Color Research and Application*, vol. 25, no. 1, February 2000.
2. Robert Rolleston, Raja Balasubramanian, "Accuracy of Various Types of Neugebauer Model", *Proc. The First IS&T/SID Color Imaging Conference*, Scottsdale, Arizona, USA, November 7-11, 1993.
3. E. J. Stollnitz, V. Ostromoukhov, D. H. Salesin, "Reproducing Color Images Using Custom Inks", Proc. of SIGGRAPH'98, in *Computer Graphics Proceedings, Annual Conference Series*, pp. 267-274, 1998.
4. K. Iino and R. S. Berns, "A Spectral Based Model of Color Printing that Compensates for Optical Interactions of Multiple Inks", AIC Color 97, *Proc. 8th Congress International Colour Association*, 1997.
5. D. Tzeng, "Spectral-Based Color Separation Algorithm Development for Multiple-Ink Color Reproduction", Ph.D Thesis, Chester F. Carlson Center for Imaging Science, College of Science, Rochester Institute of Technology, Rochester, NY, USA, 1999.
6. Marc Mahy, Paul Delebastita, "Inversion of the Neugebauer Equations", *Color Research and Application*, vol. 21, no. 6, pp. 404-411, December 1996.
7. Werner Praefcke, "Robust and fast numerical color separation for mathematical printer models", *Proc. IS&T/SID's Symposium on Electronic Imaging, Color Imaging: Device-Independent Color, Color Hard Copy and Graphics Arts III*, vol. 3648, pp.2-10, San José, California, USA, January 1999.
8. K. Iino, R. S. Berns, "Building Color-Management Modules Using Linear Optimization I. Desktop Color System", *Journal of Imaging Science and Technology*, vol. 42, no. 1, January/February 1998.
9. D. Tzeng, R. S. Berns, "Spectral-Based Six-Color Separation Minimizing Metamerism", *The Eighth IS&T/SID Color Imaging Conference*, Scottsdale, Arizona, USA, November 7-10, 2000.
10. J. A. Stephen Viggiano, "Modeling the Color of Multi-Colored Halftones", *Proc. TAGA*, p. 44-62, 1990.
11. R. Balasubramanian, "Optimization of the spectral Neugebauer model for printer characterization", *Journal of Electronic Imaging*, 8(2), 156-166, April 1999.
12. Henry R. Kang, *Color Technology for Electronic Imaging Devices*, SPIE Optical Engineering Press, Bellingham, Washington, USA, 1997.
13. W. H. Press, S. A. Teukolsky, W. T. Vetterling, B. P. Flannery, *Numerical Recipes in C*, Second Edition, Cambridge University Press.
14. D. R. Wyble, R. S. Berns, "A Critical Review of Spectral Models Applied to Binary Color Printing", *Color Research and Application*, vol. 25, no. 1, February 2000.

Spectrum Recovery from Colorimetric Data for Color Reproductions

Gaurav Sharma and Shen-ge Wang

Xerox Corp., MS0128-27E, 800 Phillips Rd., Webster, NY 14580

ABSTRACT

Colorimetric data can be readily computed from measured spectral data, however, as illustrated by metameric pairs, the mapping from spectral data to colorimetric values is many-to-one and therefore typically not invertible. In this paper, we investigate inversions of the spectrum-to-colorimetry mapping when the input is constrained to a single color reproduction medium. Under this constraint, accurate recovery of spectral data from colorimetric data is demonstrated for a number of different color reproduction processes. Applications of the spectrum reconstruction process are discussed and demonstrated through examples.

Keywords: spectral imaging, spectrum estimation, spectrum recovery, multi-spectral imaging.

1. INTRODUCTION

Human color vision is trichromatic. Under fixed viewing conditions, a color can be described by three numbers. The CIE system of colorimetry^{1,2} provides a mechanism for the standardized measurement and description of color. Given the spectral reflectance of an object and the spectral radiance of the illuminant it is viewed under, CIE colorimetry allows the color of the object to be specified as a set of *tristimulus* values. The tristimulus values can then be transformed to alternate three-dimensional color descriptions.

The three-dimensional nature of color implies that the human visual system and colorimetry systems do not resolve all differences in spectral reflectances of objects. This limitation of colorimetry is manifested in the occurrence of metameric object pairs that match under one viewing illuminant and differ under another viewing illuminant. It is commonly accepted that the transformation from spectral reflectance to colorimetry is many-to-one and therefore not invertible. Thus, while spectral reflectance data can be transformed into a three-dimensional colorimetric representation, colorimetric data for objects cannot be unambiguously transformed back to the corresponding object spectral reflectance.

While the premise that the mapping from spectral reflectance to colorimetry is many-to-one is true in general, it does not necessarily hold if the domain of spectral reflectances is restricted. Such restrictions arise naturally in image capture applications where the input is itself a reproduction. Under these situations, the mapping from spectral reflectance to colorimetry is often one-to-one and can therefore be inverted to obtain the spectral reflectance from measured colorimetry. This paper investigates several such situations that are of interest in the capture of color hardcopy images.

2. THEORETICAL BASIS FOR SPECTRUM RECOVERY

The colorimetry of a document region can be expressed in terms of its spectral reflectance and the power spectral distribution of the illuminant it is viewed under as

$$t_i = \int_{\lambda_{min}}^{\lambda_{max}} a_i(\lambda)l(\lambda)r(\lambda) d\lambda \quad i = 1, 2, 3; \quad (1)$$

where λ denotes wavelength, $\{a_1(\lambda), a_2(\lambda), a_3(\lambda)\}$ are the CIE XYZ color matching functions (CMFs),¹ $r(\lambda)$ represents the spectral reflectance of the document region, $l(\lambda)$ represents the spectral power distribution for the *viewing illuminant*, and $[\lambda_{min}, \lambda_{max}]$, represents the the interval of wavelengths outside of which all the

Authors' Email: g.sharma@ieee.org, swang@crt.xerox.com, Web: <http://chester.xerox.com/~sharma>